Spin-Wave Nonlinear Dynamics in an Yttrium Iron Garnet Sphere

Paul Bryant[a] and Carson Jeffries

Physics Department, University of California, Berkeley, California 94720, and
Materials and Chemical Sciences Division, Lawrence Berkeley Laboratory, Berkeley, California 94720

and

Katsuhiro Nakamura

Fukuoka Institute of Technology, Higashi-ku, Fukuoka 811-02, Japan
(Received 26 January 1988)

A high-resolution experiment is reported for spin-wave dynamics in an yttrium iron garnet sphere. For certain parameter values we observe a series of closely spaced spin-wave modes. Interactions between excited modes lead to various dynamical phenomena including auto-oscillations, period-doubling cascades, quasiperiodicity, and chaos. Also observed are irregular relaxation oscillations, abrupt transitions to wide-band turbulence, and hysteresis at the Suhl threshold. A theoretical model is studied analytically and numerically, explaining a number of the experimental behavior patterns.

PACS numbers: 76.50.+g, 05.45.+b, 47.20.Tg, 75.30.Ds

Spin-wave instabilities were first observed[1,2] as noisy anomalous absorption when microwave ferromagnetic absorption was strongly driven; Suhl[3] gave a theory of this behavior and remarked (1957), ". . . this situation bears a certain resemblance to the turbulent state in fluid dynamics . . .," a viewpoint recently validated by studies of spin-wave dynamics within the framework of nonlinear dynamics, which views spin waves in a ferromagnetic sphere as a set of coupled modes, with the dynamics controlled by a low-dimensional attractor. It was predicted[4] and observed[5] that excited spin waves may show a period-doubling route to chaos; further theoretical[6-10] and experimental[11-14] studies followed. We report here a high-resolution (10^{-5}) study of the first-order perpendicular pumped instability ("subsidiary absorption") in an yttrium iron garnet sphere, finding strikingly rich behavior in different regions of parameter space, including single-mode excitation; low-frequency collective oscillations when two modes are excited; quasiperiodicity, locking, and chaos when three modes are excited; and abrupt hysteretic onset of wide-band chaos at the Suhl threshold. We show that much of this behavior can be understood from stability analysis and numerical iteration of a new theoretical model of coupled modes.

In the experiment, spins on the ferrite lattice subject to fields $\mathbf{H}_0$ and $\mathbf{H}_1 \sin\omega_p t$ display a narrow ferromagnetic resonance when $\gamma H_0 = \omega_p$, with $\gamma = 1.77\times10^7$ s^{-1} and $\omega_p = 5.79\times10^{10}$ s^{-1}. In addition to this uniform precession mode, the Heisenberg exchange gives rise to spin waves.[15] A spin-wave pair, (ω_k, k) and $(\omega_k, -k)$, i.e., a "mode," is excited at half field for $\gamma H_0 = (\omega_p/2) = \omega_k$ if H_1 exceeds the Suhl threshold for the first mode to go unstable. The experiment is performed at $T = 300$ K with a sphere of pure single-crystal yttrium iron garnet (diameter $d = 0.066$ cm, spherical to 6×10^{-5}, smooth to 0.15 μm) mounted in a resonator with the crystal axis [111] $\parallel \mathbf{H}_0 \perp \mathbf{H}_1$ and incident microwave power $P_i \propto H_1^2$ from a klystron oscillator coupled via wave guide and precision attenuator. Power not absorbed is reflected to a detector, yielding a dc signal S_0 and also a low-frequency signal $S(t)$. Figure 1 shows regions and boundaries of types of observed behavior in the parameter space (P_i, H_0). As P_i and H_0 are varied, the Suhl threshold is marked by a decrease in S_0 which is abrupt (within 0.05 dB) and reversible except in the shaded area ($1200 < H_0 < 1600$ G) where it is abrupt and hysteretic, and accompanied by a large increase (50 dB) in $S(t)$ of wide-band character, with no resolvable spectral peaks. In the region $H \gtrsim 1600$ G and $P_i \approx 0.1$ dB above the Suhl threshold, we observe collective oscillations ("auto-oscillations") at 10^4 to 10^6 Hz, arising from the coupling between microwave spin-wave modes (10^{10} Hz). Their origin is revealed by a high-resolution exam-

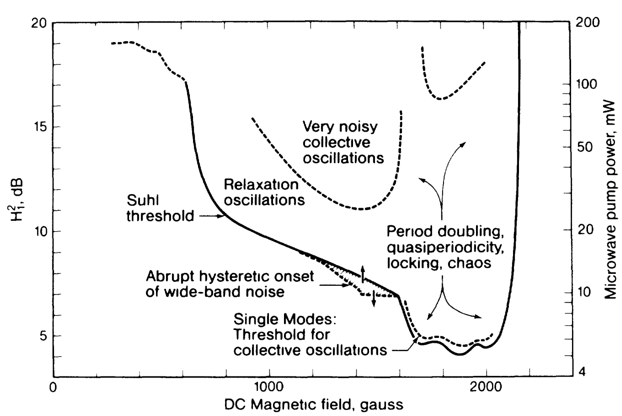

FIG. 1. Regions and boundaries of types of experimentally observed behavior in the perpendicular-pumped spin-wave instability in an yttrium iron garnet sphere; dc field H_0 vs microwave pump power $P_i \propto H_1^2$.

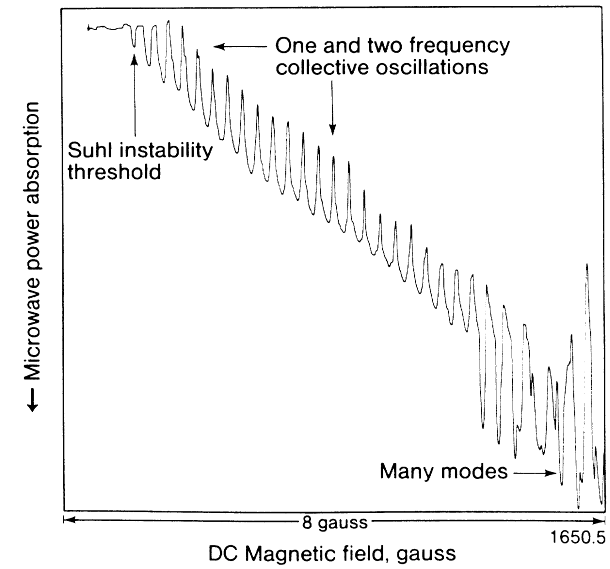

FIG. 2. Microwave absorption in an yttrium iron garnet sphere as the magnetic field is increased through the Suhl threshold, showing sequence of single spatial spin-wave modes, spaced by $\Delta H_0 \approx 0.157$ G.

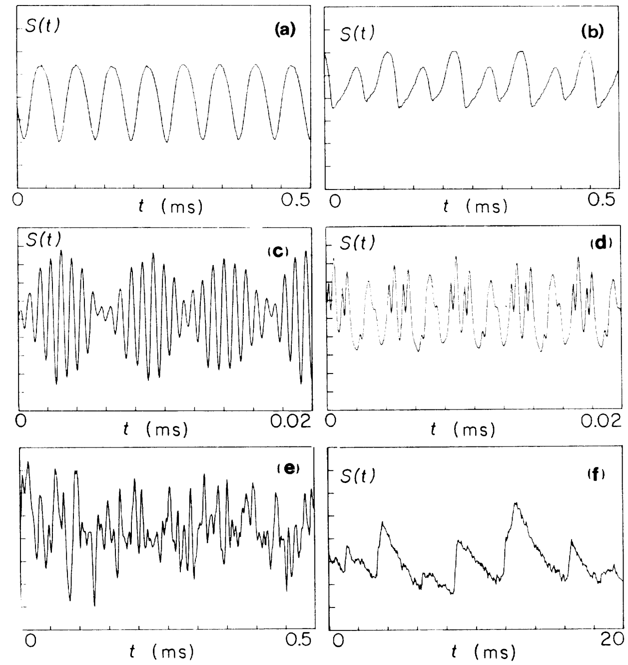

FIG. 3. Observed ac signals $S(t)$ in spin-wave instability showing (a) periodic oscillation at 16 kHz; (b) period doubled; (c) quasiperiodic; (d) frequency locking; (e) chaotic; (f) aperiodic relaxation oscillation.

ination of the Suhl threshold, showing a series of peaks (Fig. 2) separated by $\Delta H_0 = 0.157$ G; these can be understood as high-order spatial resonances of single spin-wave modes within the sphere, as originally noted by Jantz and Schneider.[16] For a small change, $\Delta k = \pi/d$, the field change computed from the dispersion relation is 0.152 G for $k = 3\times 10^5$ cm^{-1}. The first few dips in S_0 are not accompanied by an ac signal, an indication that only a single microwave mode is excited at each dip. As H_0 is increased, simultaneous excitation of two modes is possible, and a sinusoidal signal may arise [Fig. 3(a)], corresponding to a Hopf bifurcation. This collective oscillation shows period doubling [Fig. 3(b)] and sometimes a cascade to chaos [Fig. 3(e)]. The frequency f_{c0} depends partially on the dynamic interaction of the two modes and hence on P_i; the data are fitted by the expression $f_{c0}^2 = K[(P_i/P_{ic}) - 1]$, where P_{ic} is the oscillation threshold pump power; this dependence is predicted by our model and is also suggested by the work of Zautkin, L'vov, and Starobinets.[17]

These oscillations do not usually complete a cascade to chaos before interruption by the appearance of a second, incommensurate frequency f'_{c0}, [Fig. 3(c)] associated with the excitation of a third microwave mode. The system then displays quasiperiodicity, including frequency locking [Fig. 3(d)] and chaos, also predicted by the model. In the dashed-line region labeled "very noisy collective oscillations" there is a fairly abrupt onset of a higher-level base line. In yet another region of Fig. 1, we find so-called "relaxation oscillations" and irregular narrow spikes with no spectral peaks.

We model the system as a collection of coupled quantum oscillators.[18] The Hamiltonian includes the resonator mode (R), uniform mode (B), and spin waves b_k with energies ω_p, ω_0, and ω_k, respectively. These oscillators are mutually coupled with coupling constants G between R and B, g_k between B and b_k, and four-magnon interactions $T_{kk'}$, $S_{kk'}$ among $\{b_k\}$. The driving field $P_{\text{in}}^{1/2} \times \exp(-i\omega_p t)$ couples with R. From the Hamiltonian, we obtain the equations of motion for R, B, and b_k, and add phenomenological damping terms with their constants Γ, γ_0, and γ_k, respectively. We transform to slow variables C_k via $b_k = C_k \exp(-i\omega_p t/2)$ and adiabatically eliminate R,B, assuming $\Gamma \gg \gamma_k$. We assume $C_k = C_{-k}$ and arrive at a set of coupled equations for C_k as

$$\dot{C}_k = -(\gamma_k + i\Delta\Omega_k)C_k - iQg_k^* P_{\text{in}}^{1/2} C_k^* - i\sum_{k'}\{2T_{kk'}|C_{k'}|^2 C_k + (S_{kk'} + E g_{k'} g_k^*) C_{k'}^2 C_k^*\}, \tag{1}$$

where $\Delta\Omega_k \equiv \omega_k - \omega_p/2 = 2\pi\Delta f_k$ is the detuning parameter, and parameters Q and E are functions of G, ω_0, ω_p, Γ, and γ_0.

The fixed points of Eq. (1) may be determined exactly if only one mode is excited. The equation $\dot{C}_k = 0$ may be put in the form of a point on a unit circle, $M + N|C_k|^2 = (C_k^*)^2/|C_k|^2$, where $M = i(\gamma_k + i\Delta\Omega_k)/QP_{\text{in}}^{1/2} g_k^*$, and $N = -(2T_{kk} + S_{kk} + E|g_k|^2)/QP_{\text{in}}^{1/2} g_k^*$. The Suhl threshold occurs at $|M| = 1$. For $P_{\text{in}} > P_t$ (P_t = threshold power)

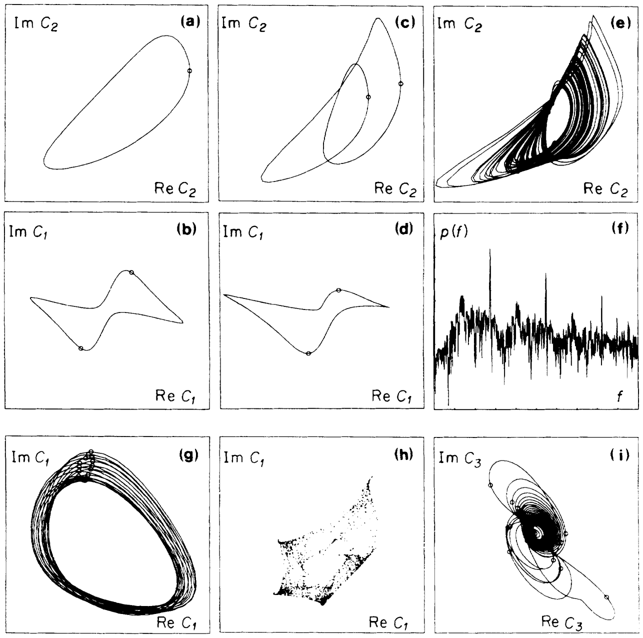

FIG. 4. (a) Computed behavior for two modes: phase portrait for periodic oscillations, asymmetric mode; $\Delta f_1 = -300$ kHz, $\Delta f_2 = 200$ kHz. (b) Symmetric mode. (c) Period doubling of asymmetric mode; $\Delta f_1 = -385$ kHz, $\Delta f_1 = 115$ kHz. (d) Symmetry breaking of symmetric mode. (e) Chaotic orbit following period doubling cascade; $\Delta f_1 = -410$ kHz, $\Delta f_2 = 90$ kHz. (f) Power spectrum of chaotic orbit, $f_{\max} = 2.5$ MHz. (g) Computed phase portrait for quasiperiodic behavior for three modes, with Poincaré section. (h) Poincaré section of chaotic orbit; proximity to period-5 locking produces the five points. (i) Chaotic bursts.

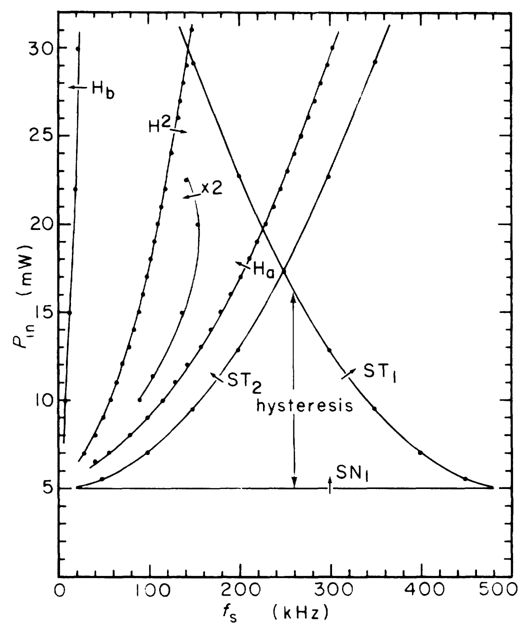

FIG. 5. Computed parameter-space diagram for the model, Eq. (1), for up to three active modes.

the stability of the trivial fixed point ($C_k = 0$) is lost in a symmetry-breaking bifurcation. This occurs in two forms: (1) If $\mathrm{Re}(M/N) > 0$, one obtains a supercritical bifurcation in which stable nonzero fixed points emerge from the origin as P_{in} crosses P_t. (2) For $\mathrm{Re}(M/N) < 0$ a subcritical bifurcation occurs in which stable nonzero fixed points appear below P_t, and the system will jump to these at $P_{in} = P_t$, resulting in hysteretic behavior. The experimentally observed hysteresis is probably a related effect involving the cooperation of neighboring modes.

To explore the behavior of Eq. (1) we perform a numerical iteration[19] for $N=1$, then $N=2$, etc. For $N=1$, the system is always attracted to a fixed point, but a hysteresis may be displayed as noted above. For $N=2$, periodic oscillations are found [Figs. 4(a) and 4(b)]: Mode 2 exhibits an asymmetric orbit while mode 1 exhibits a symmetrical orbit at twice the period. We simulate the spatial modes of Fig. 2 by choosing $\Delta f_1 = f_s - 500$ kHz and $\Delta f_2 = f_s$, and shift f_s to simulate the dc field shift. The computed behavior [Figs. 4(c) and 4(d)] shows period doubling and symmetry breaking, respectively, and eventually chaotic behavior [Figs. 4(e) and 4(f)] for both modes.

For $N=3$ modes, new behavior arises: Figure 4(g) shows quasiperiodic behavior with a smooth Poincaré section of a torus; at higher excitation the section [Fig. 4(h)] is a chaotic attractor. For some other parameter values the behavior shows chaotic bursts [Fig. 4(i)] and other forms of aperiodic behavior similar to that observed [Fig. 3(f)]. The computed behavior in parameter space (P_{in}, f_s) is shown in Fig. 5 for active participation of one, two, or three modes ($\Delta f_3 = f_s + 500$ kHz). The boundaries ST and SN are the absorption thresholds for increasing and decreasing P_{in}, respectively, showing hysteresis; H_a is the boundary for a Hopf bifurcation to a limit cycle which shows period doubling at the $\times 2$ boundary; the line H^2 is a secondary Hopf bifurcation to quasiperiodicity involving modes 1, 2, and 3; in the upper central region we find more exotic behavior.

To summarize, these new experimental findings for the first-order perpendicular pumping exhibit rich structures comparable to those of chaos and turbulence in fluid dynamics. These results, together with numerical computations from the model, give a surprisingly good picture of spin-wave dynamics in the chaotic regime.

This work was supported in part by the U.S. Department of Energy under Contract No. DE-AC03-76SF00098, and by the U.S. Office of Naval Research under Contract No. N00014-86-K-0154.

[a]Present address: Institute for Pure and Applied Physical Sciences, University of California, San Diego, La Jolla, CA 92093.

[1]R. W. Damon, Rev. Mod. Phys. **25**, 239 (1953).
[2]N. Bloembergen and S. Wang, Phys. Rev. **93**, 72 (1954).
[3]H. Suhl, J. Phys. Chem. Solids **1**, 209 (1957).
[4]K. Nakamura, S. Ohta, and K. Kawasaki, J. Phys. C **15**, L143 (1982), and J. Phys. Soc. Jpn. **52**, 147 (1983).
[5]G. Gibson and C. Jeffries, Phys. Rev. A **29**, 811 (1984).
[6]S. Ohta and K. Nakamura, J. Phys. C **16**, L605 (1983).
[7]X. Y. Zhang and H. Suhl, Phys. Rev. A **32**, 2530 (1985); H. Suhl and X. Y. Zhang, Phys. Rev. Lett. **57**, 1480 (1986).
[8]S. M. Rezende, O. F. de Alcontara Bonfin, and F. M. de Aguiar, Phys. Rev. B **33**, 5153 (1986).
[9]X. Y. Zhang and H. Suhl, to be published.
[10]F. Waldner, D. R. Barberis, and H. Yamazaki, Phys. Rev. A **31**, 420 (1985).
[11]F. M. de Aguiar and S. M. Rezende, Phys. Rev. Lett. **56**, 1070 (1986).
[12]M. Mino and H. Yamazaki, J. Phys. Soc. Jpn. **55**, 4168 (1986); H. Yamazaki and M. Warden, J. Phys. Soc. Jpn. **55**, 4477 (1986).
[13]T. L. Carroll, L. M. Pecora, and F. J. Ratchford, Phys. Rev. Lett. **59**, 2891 (1987).
[14]P. H. Bryant, Ph.D. thesis, University of California, 1987 (unpublished).
[15]A. M. Clogston, H. Suhl, L. R. Walker, and P. W. Anderson, J. Phys. Chem. Solids **1**, 129 (1956).
[16]W. Jantz and J. Schneider, Phys. Status Solidi (a) **31**, 595 (1975).
[17]V. V. Zautkin, V. S. L'vov, and S. S. Starobinets, Zh. Eksp. Teor. Fiz. **63**, 182 (1973) [Sov. Phys. JETP **36**, 96 (1973)].
[18]P. H. Bryant, C. D. Jeffries, and K. Nakamura, to be published.
[19]Typical parameter values used: $P_{\mathrm{in}}=0.015$ W; $\gamma_k=1\times10^6$ s^{-1}; $iQg_k=1.414\times10^7$ $\mathrm{W}^{-1/2}\,\mathrm{s}^{-1}$; $S_{kk'}=S_{kk}=4.3\times10^{-8}$ s^{-1}; $T_{kk'}=-2\times10^{-8}$ s^{-1}; $T_{kk}=0$; $E=0$.

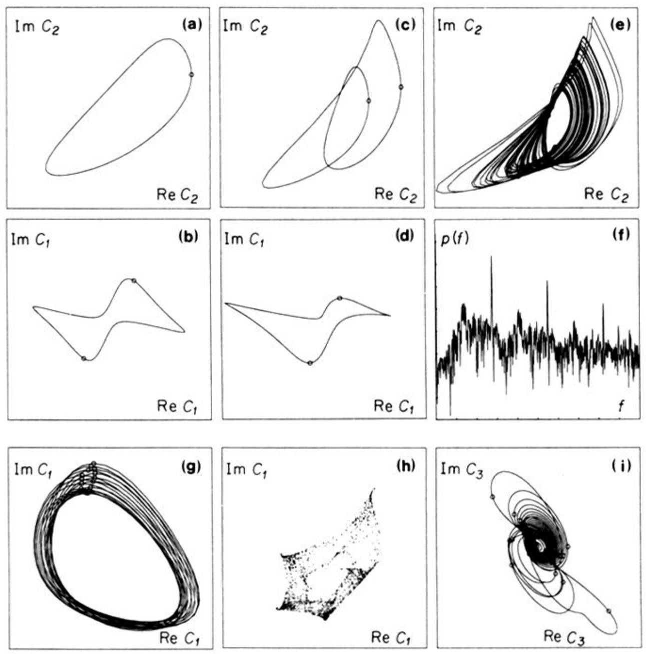

FIG. 4. (a) Computed behavior for two modes: phase portrait for periodic oscillations, asymmetric mode; $\Delta f_1 = -300$ kHz, $\Delta f_2 = 200$ kHz. (b) Symmetric mode. (c) Period doubling of asymmetric mode; $\Delta f_1 = -385$ kHz, $\Delta f_1 = 115$ kHz. (d) Symmetry breaking of symmetric mode. (e) Chaotic orbit following period doubling cascade; $\Delta f_1 = -410$ kHz, $\Delta f_2 = 90$ kHz. (f) Power spectrum of chaotic orbit, $f_{\mathbf{max}} = 2.5$ MHz. (g) Computed phase portrait for quasiperiodic behavior for three modes, with Poincaré section. (h) Poincaré section of chaotic orbit; proximity to period-5 locking produces the five points. (i) Chaotic bursts.